



FORC analysis of Ni(SiO₂) nanogranular film in the blocked regime

R. Lavín^{a,b}, C. Farías^b, J.C. Denardin^{a,c,*}

^a Departamento de Física, Universidad de Santiago de Chile, USACH, Av. Ecuador 3493, Santiago, Chile

^b Facultad de Ingeniería, Universidad Diego Portales, UDP, Ejército 441, Santiago, Chile

^c Centro para el Desarrollo de la Nanociencia y la Nanotecnología, CEDENNA, Av. Ecuador 3493, Santiago, Chile

ARTICLE INFO

Article history:

Received 14 September 2011

Received in revised form

8 December 2011

Available online 14 January 2012

Keywords:

Magnetic nanoparticle

FORC diagram

Size distribution

ABSTRACT

In this work the magnetic and structural properties of granular Ni(SiO₂) films are studied by means of FORCs diagrams and microscopy. Transmission electron microscopy images show that the sample is composed of a fine dispersion of Ni nanoparticles with 3.7 nm in average sizes. Magnetic measurements as function of temperature show that the nanoparticles are superparamagnetic at room temperature and are blocked at 5 K. The FORCs diagrams obtained below the blocking temperature allow us to determine the average size of the nanoparticles and the distribution of sizes in a very good agreement with TEM images.

© 2012 Elsevier B.V. All rights reserved.

1. Introduction

In recent decades the study of nanostructured magnetic systems has attracted considerable interest owing to their interesting physical properties and technological applications. The synthesis of magnetic nanoparticle arrays with a controlled morphology is very important for applications in information storage devices [1,2], among other applications [1,3]. Measuring the hysteresis curve is the most commonly used technique in the study of global magnetic properties. However, it is not possible from the analysis of the curves to clarify all the aspects of these complex systems. In this context, the FORCs (first order reversal curves) diagram technique is a powerful tool in the characterization of magnetic systems [4–6]. This technique is already being used to study the coexistence of different magnetization reversal modes in magnetic nanodot arrays [7,8], on arrays of nanowires and other magnetic systems [9–11]. The FORCs diagram of these systems provides information about the distribution of coercivity and interaction of the particles and the portion of reversible and irreversible magnetization that is present in the system [12]. In this work the morphological and magnetic properties of granular Ni(SiO₂) films have been studied. Magnetic measurements as function of temperature and FORCs diagrams give hints on aspects of the magnetic regime, as distribution of coercivities, interactions and size of nanoparticles.

2. Experimental details

The granular Ni(SiO₂) films have been prepared in a magnetron co-sputtering system, with the transition metal and SiO₂ targets mounted on two separate guns. The glass substrates were rotated during sputtering, to ensure composition uniformity and a random distribution of easy axes of the nanoparticles. The metal volume fraction was controlled by the relative sputtering rates, and then determined by energy-dispersive X-ray spectroscopy using a Philips EDAX XL30 on films deposited in the same run on Kapton. The samples deposited on Kapton were used for magnetic measurements. Structural characterization was performed, using a Transmission Electron Microscope (TEM) Jeol JEM-3010 ARP, and reveal a structure with extremely fine dispersion of Ni metal nanoparticles embedded in an insulating matrix. Magnetic properties as function of field and temperature were measured in a Superconducting Quantum Interference Device (SQUID) system in the temperature range 5–300 K.

3. Results and discussion

Fig. 1(a) shows that the film is composed of nanoparticles immersed in an insulating matrix. In Fig. 1(b) it is possible to observe that the Ni nanoparticles are small and are not touching with each other. The average size of the particles and the dispersion of nanoparticle sizes were obtained measuring the particle sizes in different parts of the sample, and is shown in Fig. 1(c). The size distribution has been adjusted by a log-normal distribution, obtaining an average diameter of 3.7 nm. One can expect that at ambient temperature the nanoparticles have a superparamagnetic behavior. To corroborate this, the hysteresis

* Corresponding author at: Departamento de Física, Universidad de Santiago de Chile, USACH, Av. Ecuador 3493, Santiago, Chile. Tel.: +56 2 7181256.

E-mail address: juliano.denardin@usach.cl (J.C. Denardin).

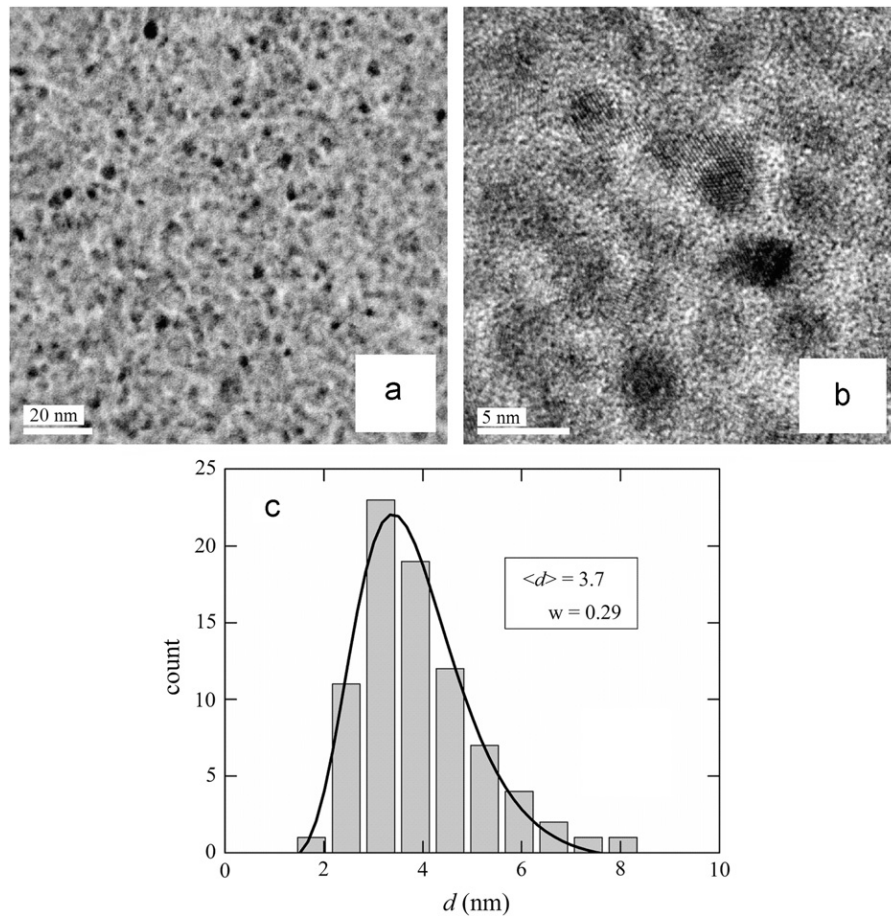


Fig. 1. (a) TEM image of a Ni(SiO₂) film. (b) High resolution TEM image of the same sample and (c) Size distribution of the particles and adjusted log-normal function, which gives an average diameter of 3.7 nm.

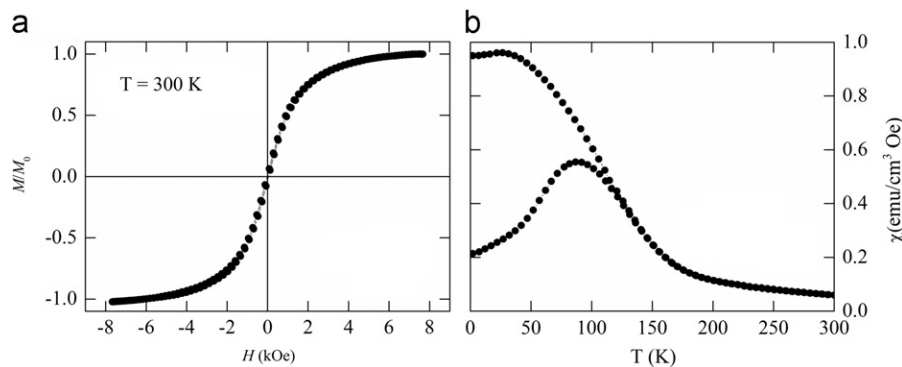


Fig. 2. (a) Hysteresis curve of Ni nanoparticles at 300 K and (b) ZFC and FC curves of the same sample.

curve was measured at ambient temperature, (see Fig. 2(a)), and shows characteristics of a superparamagnetic system; with zero coercivity and remanence. Fig. 2(b) shows zero-field-cooling (ZFC) and field-cooling (FC) curves in the range of 5 to 300 K. Considering the average blocking temperature of the system as the maximum of the ZFC curve, an average blocking temperature of approximately 87 K can be estimated for the nanoparticles. One can also note that the temperature where the ZFC/FC curves separate is larger (above 100 K). The difference in temperatures of the maximum of the ZFC and bifurcation of the curves is proportional to the dispersion of sizes in the sample. The effect of the size of the nanoparticles strongly influences the coercivity

since small variations in diameters can define if a nanoparticle is in the blocked regime or in the superparamagnetic regime.

In order to study the magnetic behavior of this system in more detail it was necessary to decrease the temperature well below the blocking temperature, where the hysteresis curves present coercivity and remanence. A detailed magnetic characterization by means of FORCs and FORCs diagrams was made at 5 K. Measuring a FORC begins by saturating the sample to a high field. The field is then reduced to a H_a reversal field. Thus, FORC is defined as the magnetization curve measured when the applied field increases from H_a until saturation. Magnetization for the H_b field over the FORC with the initial H_a field is denoted by $M(H_a, H_b)$,

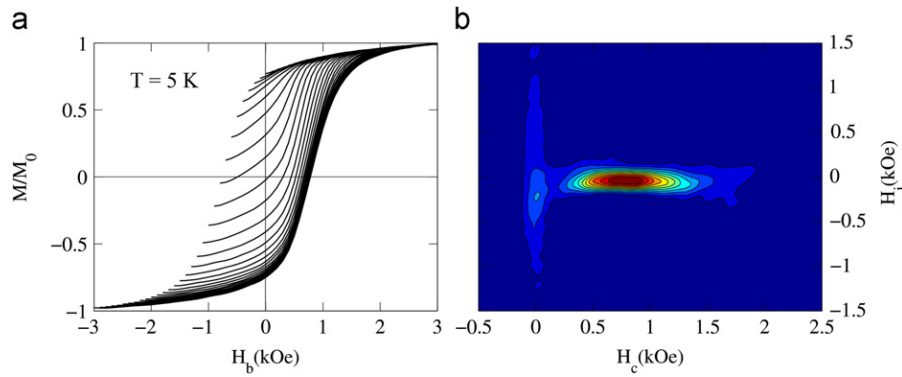


Fig. 3. (a) FORCs measured with a SQUID at 5 K and (b) corresponding FORC diagram obtained by numeric derivation.

where $H_b > H_a$. A statistical model that describes the system as a set of magnetic entities based on the Preisach model [4] is used to illustrate and obtain information from the FORCs. The probability density function of the ensemble is defined by [5]

$$\rho(H_a, H_b) = -\frac{1}{2} \frac{\partial^2 M}{\partial H_a \partial H_b} \quad (1)$$

This function extends over the entire H_a , H_b plane. A FORCs diagram is a contour plot of (Eq. (1)), and can be expressed in terms of the variables $H_c = (H_b - H_a)/2$ and $H_i = (H_b + H_a)/2$, which are the commutation (coercivity of an entity) and interaction fields (shift of an entity) [5,13], allowing us to capture the reversible magnetization component, which appears to be centered in $H_c = 0$. The density function (Eq. (1)) for a sample is obtained by numeric derivation of the $M(H_a, H_b)$ function, which contains all the measured FORCs. The FORCs diagram is obtained by making a contour plot of the Eq. (1).

Fig. 3(a) shows the FORCs for the sample at a temperature of 5 K. The hysteresis curve delineated by the external contour of the FORCs corresponds exactly to the hysteresis curve of the sample. The Ni nanoparticles at 5 K exhibit a regular hysteresis curve characteristic of a ferromagnetic system, with a coercivity of 850 Oe and reduced remanence M_r/M_0 , of 0.76, in contrast to the superparamagnetic hysteresis curve at 300 K (Fig. 2(a)). The FORCs diagram obtained from numeric derivation of the FORCs in Fig. 3(a) is shown in Fig. 3(b). At 5 K, a narrow crest can be observed in the diagram, centered at $H_c = 0$ Oe, which corresponds to the reversible magnetization component. Together with the reversible magnetization component, for $H_c > 0$ Oe, a single narrow ridge is observed along the coercivity axis, H_c , which corresponds to the irreversible magnetization component. This single high coercivity magnetic phase represents the particles in the blocked regime. The regular and elongated narrow shape of the high coercivity phase in the H_i axis reveals the presence of a system composed of particles with limited distribution of interaction fields and a wide distribution of coercivity fields. This pattern is characteristic of a system composed of an ensemble of single-domain particles with small interactions and a wide size distribution [4]. The maximum of this phase is centered on the H_c axis in 817 Oe, close to the coercivity values of the hysteresis curve 850 Oe, and on the H_i axis close to 0 Oe, demonstrating that the system is composed largely of an ensemble of non-interacting magnetic nanoparticles. The distribution of coercivity of the nanoparticles observed in the FORCs diagram is itself another evidence of the existence of a size distribution of the nanoparticles.

Fig. 4 shows the coercivity distribution extracted from the FORCs diagram, where the reversible and irreversible magnetization components can be observed. The coercivity of spherical

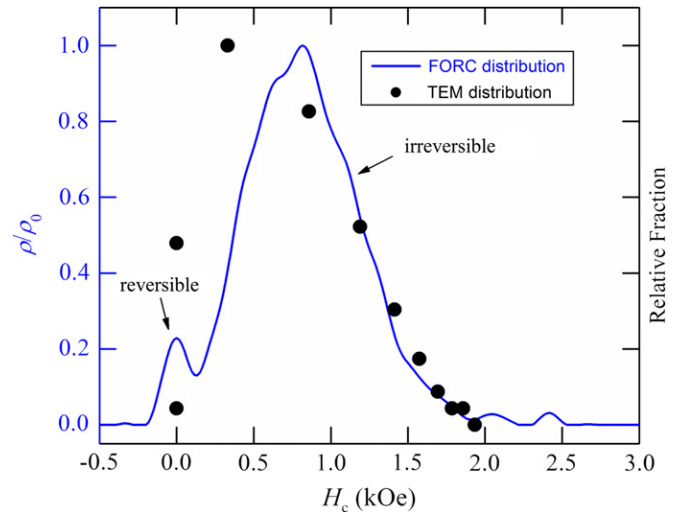


Fig. 4. (Continuous line) Coercivity distribution for the interaction field $H_i = 0$ Oe, that is, $\rho(H_c, H_i = 0)/\rho_0$, extracted from the FORC diagram, and (dots) coercivity distribution obtained with expression (2) based on the size distribution obtained from the electron microscope (TEM).

particles with uniaxial anisotropy, which reverts its magnetization in a completely coherent manner, is given by the expression

$$H_c = C_1 - \frac{C_2}{d^{3/2}}, \quad (2)$$

where d is the diameter of the particle, $C_1 = 2K/M_0$ and $C_2 = C_1(150 \text{ kT}/\pi K)^{1/2}$ are constants that depend on the material microscopic parameters and the temperature T [14], where k is the Boltzmann constant, K is the crystalline anisotropy constant, and M_0 is the saturation magnetization. Here we used the values of constants at $T = 5$ K of $K = -12 \times 10^4 \text{ J/m}^3$ and $M_0 = 5 \times 10^5 \text{ A/m}$. In this way, we can compare the distribution of coercivity of the FORCs diagram, with the coercivity distribution obtained with expression (2) and the size distribution from the TEM (Fig. 1(c)). This last distribution of coercivity is obtained by assigning to each value of $H_c(d)$, calculated with the expression (2), the corresponding weight of the size distribution of Fig. 1(c). The points in Fig. 4 are the distribution obtained with expression (2), showing good agreement with the coercivity distribution of the FORCs diagram. The divergence of the curves for small values of coercivity (smaller particles) can be explained by some presence of dipolar interactions that are not considered in this approximation. Despite this, the FORCs diagram gives us the correct order of magnitude of the nanoparticle sizes. Calculating the particle diameter for the maximum of the FORCs coercivity distribution

(for 817 Oe), we obtain the value of $d=3.4$ nm, which represents the average diameter of the nanoparticles, with good agreement with the value of 3.7 nm obtained with TEM (Fig. 1(c)).

4. Conclusion

In this work we have studied the magnetic and structural properties of Ni nanoparticles dispersed in an insulating matrix by means of microscopy, magnetization and FORCs diagrams. By measuring FORCs of the film at low temperature we have been able to determine the average size and the dispersion of the nanoparticles with a very good agreement with microscopy images. The FORCs analyses also give us important information about the presence of dipolar interactions in the system. The FORCs technique is a tool that can be used to unveil structural characteristics of complex magnetic systems.

Acknowledgments

This work was supported by the Fondecyt Grants 3100117 and 1110252. Financiamiento Basal para Centros Científicos y Tecnológicos de Excelencia FB0807, AFOSR FA9550-11-1-0347, and

Millennium Science Nucleus Basic and Applied Magnetism P10-061F.

References

- [1] V. Skumryev, S. Stoyanov, Y. Zhang, G. Hadjipanayis, D. Givord, J. Nogues, *Nature* 423 (2003) 850.
- [2] D. Kong, C. Chen, L. He, *Journal of Applied Physics* 103 (2008) 114312.
- [3] J.C. Denardin, M. Knobel, X.X. Zhang, A.B. Pakhomov, *Journal of Magnetism and Magnetic Materials* 262 (2003) 15–22.
- [4] C.R. Pike, A.P. Roberts, K.L. Verosub, *Journal of Applied Physics* 85 (1999) 6660–6667.
- [5] C.R. Pike, *Physical Review B* 68 (2003) 104424.
- [6] C.R. Pike, C.A. Ross, R.T. Scalettar, G. Zimanyi, *Physical Review B* 71 (2005) 134407.
- [7] R.K. Dumas, Ch.-P. Li, I.V. Roshchin, I.K. Schuller, K. Liu, *Physical Review B* 75 (2007) 134405.
- [8] C. Pike, A. Fernandez, *Journal of Applied Physics* 85 (1999) 6668.
- [9] H. Chiriac, N. Lupu, L. Stoleriu, P. Postolache, A. Stancu, *Journal of Magnetism and Magnetic Materials* 316 (2007) 177–180.
- [10] R. Lavín, B. Torres, D. Serafini, J.C. Denardin, *Molecular Crystals and Liquid Crystals* 521 (2010) 279–287.
- [11] R. Lavín, J.C. Denardin, J. Escrig, D. Altbir, A. Cortés, H. Gómez, *IEEE Transactions on Magnetics* 44 (2008) 2808–2811.
- [12] F. Béron, D. Ménard, A. Yelon, *Journal of Applied Physics* 103 (2008) 07D908.
- [13] G. Bertotti, *Hysteresis in Magnetism*, Academic Press, NY, USA, 1998.
- [14] B.D. Cullity, C.D. Graham, *Introduction to Magnetic Materials*, IEEE Press, 2009.